

# Anomalous diffusion of oligomerized transmembrane proteins

Ulrich Schmidt<sup>1,2</sup> and Matthias Weiss<sup>2,3,a)</sup>

<sup>1</sup>Laboratory for Computational Cell Biology, Department of Cell Biology, Harvard Medical School, Massachusetts 02115, USA

<sup>2</sup>Cellular Biophysics Group, German Cancer Research Center, D-69120 Heidelberg, Germany

<sup>3</sup>Experimental Physics I, University of Bayreuth, D-95440 Bayreuth, Germany

(Received 23 November 2010; accepted 5 April 2011; published online 22 April 2011)

Transmembrane proteins frequently form (transient) oligomers on biomembranes, e.g., while participating in protein sorting and signaling events. Using coarse-grained membrane simulations we show here that transmembrane proteins show a subdiffusive motion on short time scales when being part of a linear oligomer, i.e., a flexible polymer, embedded in a two-dimensional membrane. Our results are in agreement with previous experimental observations. They further indicate that polymers of transmembrane proteins are well described by predictions from Rouse theory in two dimensions even in the presence of hydrodynamic interactions. © 2011 American Institute of Physics. [doi:10.1063/1.3582336]

## I. INTRODUCTION

Membrane proteins frequently assemble into higher-order structures, e.g., clusters or linear polymers, to modulate their function, to regulate their trafficking, and to achieve or maintain their proper subcellular localization.<sup>1,2</sup> A prominent example are p24 proteins that form heterooligomers to facilitate their trafficking along the cell's secretory pathway.<sup>3</sup> The oligomer's structure determines in particular the diffusion of the assembly's center of mass and, more importantly, that of the participating monomers. Indeed, many advanced light microscopy techniques, e.g., fluorescence correlation spectroscopy or single molecule tracking, measure only the mean square displacement (MSD) of single or few labeled monomers within an oligomer, hence reporting mainly on the monomers' diffusion properties. Owing to this experimental constraint, any interpretation of experimentally determined (anomalous) diffusion requires additional theoretical considerations.

Anomalous diffusion (or to be more precise: subdiffusion) is characterized by a nonlinear scaling of the MSD, i.e.,  $\langle r^2(t) \rangle \sim t^\alpha$  with  $\alpha < 1$ . It is frequently observed on biomembranes<sup>4-7</sup> and in complex fluids<sup>8-11</sup> as a transient scaling over several orders of magnitude. Several microscopic origins for the emergence of subdiffusion have been studied intensively, e.g., obstructed diffusion,<sup>12</sup> fractional Brownian motion,<sup>13</sup> or continuous time random walks,<sup>14</sup> but whether any of these models is the basis for the experimentally observed subdiffusion in living cells is still a matter of discussion.<sup>15-17</sup>

A particular scenario in which (transient) subdiffusion is also anticipated is the motion of monomers in polymers. While subdiffusion of monomers is a well-established phenomenon in bulk solution,<sup>18,19</sup> the situation is much less clear in two dimensions, e.g., when transmembrane proteins oligomerize to form an effective polymer (cf. Fig. 1). While

self-avoidance leads to a radius of gyration (within the membrane) that scales as  $R_g \sim N^\nu$  with  $\nu = 3/4$  being the Flory exponent, the monomer's diffusion properties depend critically on the chosen polymer model. Neglecting hydrodynamic interactions and respecting only self-avoidance (Rouse model), monomers are predicted to show an MSD  $\langle r^2(t) \rangle \sim t^\alpha$  with  $\alpha = 3/5$  (Ref. 20) while including hydrodynamic interactions leads to the prediction that monomers always show normal diffusion ( $\alpha = 1$ ) with their MSD being congruent to that of the polymer's center of mass.<sup>20</sup>

To our knowledge, there is no comprehensive theory that treats the dynamics of a polymer embedded in a two-dimensional sheet that is surrounded by a bulk fluid. However, a recent theoretical study<sup>21</sup> investigated polymer motion in sheetlike cavities and postulated a Rouse-like behavior of experimental observables due to symmetry properties of the Oseen tensor. While this result was strictly derived only for polymer motion in a thin slab between two hard walls, the study concluded that Rouse-like behavior should also occur when the walls are soft.

Here we show by means of coarse-grained simulations that individual transmembrane proteins that are part of a membrane-resident linear polymer indeed show subdiffusive motion. This result compares favorably to previous experimental observations on the subdiffusion of transmembrane glycosylation enzymes in the endoplasmic reticulum and in the Golgi apparatus.<sup>6</sup> Albeit the simulation approach naturally includes hydrodynamic interactions, the emergence of monomer subdiffusion highlights that membrane-bound polymers follow a Rouse-like rather than a Zimm-like behavior. Finally, we demonstrate that the center-of-mass diffusion of the polymer is well captured by the Saffman–Delbrück relation for globular membrane inclusions.

## II. SIMULATIONS

For our simulations, we have used dissipative particle dynamics (DPD). In accordance with standard DPD

<sup>a)</sup> Author to whom correspondence should be addressed. Electronic mail: matthias.weiss@uni-bayreuth.de.

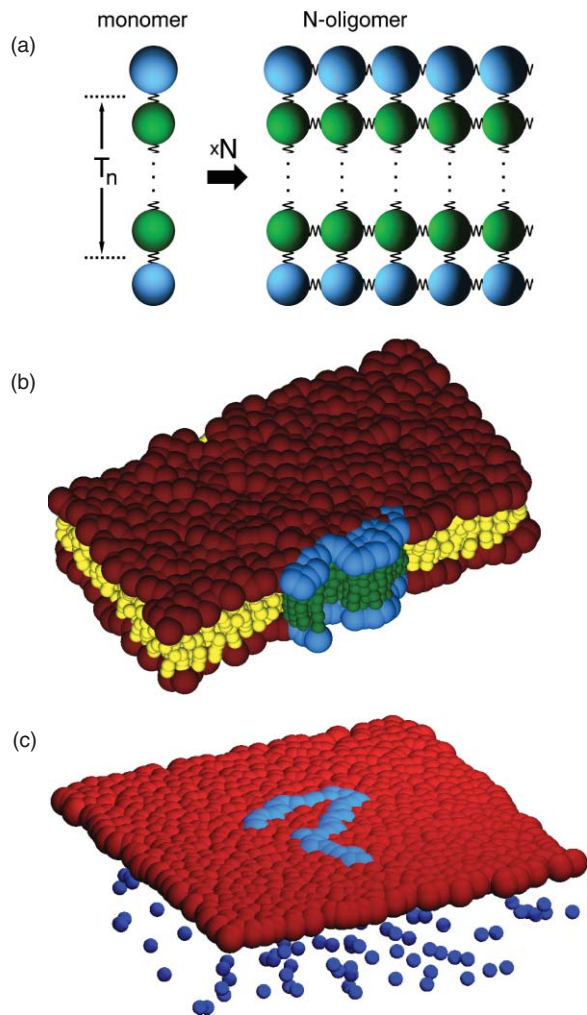


FIG. 1. (a) Model of a single transmembrane protein with  $n$  hydrophobic beads (left), and a linear polymer of these proteins (right); see main text for a detailed description. (b) Model of a linear polymer ( $N = 32$ ) of transmembrane proteins embedded in a fluid membrane. Proteins have  $n = 5$  transmembrane layers, solvent particles are not shown. (c) Model of a linear polymer ( $N = 32$ ) embedded in a thin fluid film ( $z$ -coordinate fixed; cf. main text for details). A small number of solvent particle is also shown.

models,<sup>22–24</sup> we have imposed a linear repulsive force  $\mathbf{F}_{ij}^C = a_{ij}(1 - r_{ij}/r_0)\hat{\mathbf{r}}_{ij}$  between any two beads  $i, j$  having a distance  $r_{ij} = |\mathbf{r}_{ij}| = |\mathbf{r}_i - \mathbf{r}_j| \leq r_0$  (with  $\hat{\mathbf{r}}_{ij} = \mathbf{r}_{ij}/r_{ij}$  denoting the corresponding unit vector). The degree of hydrophobicity was tuned via the interaction energies  $a_{ij}$  while bonds within lipids and proteins were modeled via a harmonic potential  $U(\mathbf{r}_i, \mathbf{r}_{i+1}) = k(r_{i,i+1} - l_0)^2/2$  between the respective beads. Lipids and proteins were given an additional bending stiffness via the potential  $V(\mathbf{r}_{i-1}, \mathbf{r}_i, \mathbf{r}_{i+1}) = \kappa[1 - \cos(\phi)]$  with  $\cos \phi = \hat{\mathbf{r}}_{i-1,i} \cdot \hat{\mathbf{r}}_{i,i+1}$ . For the thermostat, dissipative and random forces were given by  $\mathbf{F}_{ij}^D = -\gamma_{ij}(1 - r_{ij}/r_0)^2(\hat{\mathbf{r}}_{ij} \cdot \mathbf{v}_{ij})\hat{\mathbf{r}}_{ij}$  and  $\mathbf{F}_{ij}^R = \sigma_{ij}(1 - r_{ij}/r_0)\zeta_{ij}\hat{\mathbf{r}}_{ij}$ , respectively, when  $r_{ij} \leq r_0$ . Here,  $\mathbf{v}_{ij} = \mathbf{v}_i - \mathbf{v}_j$  denotes the relative velocity between the particles  $i, j$  while  $\zeta_{ij}$  is a random variable with  $\langle \zeta_{ij} \rangle = 0$  and  $\langle \zeta_{ij}\zeta_{kl} \rangle = \delta_{ik}\delta_{jl}$ . The parameters  $\gamma_{ij}$  and  $\sigma_{ij}$  are related via the fluctuation–dissipation theorem  $\sigma_{ij}^2 = 2\gamma_{ij}k_B T$ .<sup>23</sup>

The interaction cutoff  $r_0$ , the bead mass  $m$  (all beads were assumed to have the same mass), and the thermo-

stat temperature  $k_B T$  were set to unity. In accordance with Ref. 25 we have chosen  $\sigma_{ij} = 3$ ,  $\gamma_{ij} = 9/2$ ,  $k = 100k_B T/r_0^2$ ,  $l_0 = 0.45r_0$ ,  $\kappa = 10k_B T$ ,  $a_{HT} = a_{WT} = 200k_B T$ , and  $a_{WW} = a_{HH} = a_{TT} = a_{WH} = 25k_B T$  (subscripts W, H, and T denoting water, lipid head, and lipid tail bead, respectively). Lipids were modeled as a linear chain (HT<sub>3</sub>), while proteins were modeled as single HT <sub>$n$</sub> H chains [Fig. 1(a)]. By linking these HT <sub>$n$</sub> H proteins in lateral direction via harmonic bonds ( $k$  and  $l_0$  as above), we created flexible, linear oligomers of size  $N = 4, 8, 16$ , and  $32$  that were integrated into a fully hydrated model membrane [cf. Figs. 1(a) and 1(b)]. The length of the model membrane in  $xy$ -direction was set to  $L = 20r_0$  for  $N = 4, 8, 16$  and  $L = 25r_0$  for  $N = 32$ . These settings minimize finite-size effects, yet allow for reasonable computation times. Choosing Hookean springs as a model for tethering transmembrane proteins implies that realistic potentials between these proteins are only taken into account to harmonic order. Moreover, we tacitly assume by this approach that the attractive potential between proteins is strong enough that a dissociation occurs only beyond the time scales that are simulated here.

We have integrated the equations of motion with a velocity Verlet scheme<sup>26</sup> (time increment  $\Delta t = 0.01$ ) using periodic boundary conditions. To achieve a tensionless membrane, we first equilibrated the system for  $5 \times 10^4$  steps with a barostat<sup>27</sup> and then fixed the length of the simulation box for the remaining  $1.5 \times 10^6$  simulation steps. The intrinsic DPD units may be converted to SI units ( $r_0 \equiv 1$  nm,  $\Delta t \equiv 80$  ps) by gauging the membrane thickness and the lipids' diffusion coefficient.<sup>28</sup>

To complement our results obtained for a free-standing, hydrated membrane, we also employed a setup that has been used before to study the dynamics of phase separations in thin liquid films.<sup>29</sup> Here, the membrane is modeled as a single layer of beads with a fixed  $z$ -component, i.e., beads (free or being part of a polymer) can move laterally but undulations of the membrane are suppressed. A polymer within the membrane simply consisted of  $N$  beads connected via Hookean springs [cf. Fig. 1(c)]; all parameters as noted above. It has been shown earlier that this setup faithfully can reproduce the two-dimensional dynamics and is only mildly perturbed by local cooling.<sup>29</sup> Here, we modeled linear polymers of length  $N = 4, 8, 16, 32, 64$ , and  $128$  embedded in thin liquid sheets of size  $L = 20r_0$  for  $N \leq 16$  and  $L = 25, 30$ , and  $35r_0$  for  $N = 32, 64$ , and  $128$ , respectively.

### III. RESULTS AND DISCUSSION

We first inspected the scaling of the polymer's radius of gyration  $R_g$  as a function of the number  $N$  of participating transmembrane proteins, and the length  $n$  of the proteins' transmembrane domain. We have shown previously that  $n = 5$  in the chosen simulation setup yields the best match between the hydrophobic domain of the proteins and the hydrophobic core of the lipid bilayer.<sup>30</sup> Increasing or reducing  $n$  leads to a hydrophobic mismatch, i.e., the protein's hydrophobic moiety is too long or too short to be accommodated by the unperturbed lipid bilayer. The resulting local perturbation of the bilayer leads to a clustering of

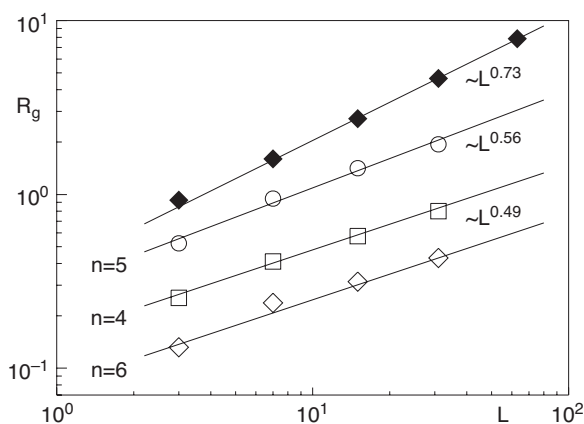


FIG. 2. The scaling of the radius of gyration of a polymer of transmembrane proteins is in good agreement with the prediction for a two-dimensional molten globule ( $R_g \sim L^{1/2}$ ) when proteins exhibit a strong hydrophobic mismatch with the surrounding lipid bilayer ( $n = 4$  and  $6$ ). The scaling tends toward the anticipated scaling for a Flory polymer in two dimensions ( $R_g \sim L^{3/4}$ ) when the mismatch is almost vanishing ( $n = 5$ ). An even better agreement with the Flory scaling is seen when the membrane is modeled as a thin liquid film (filled symbols; see main text for details). Curves for  $n = 4, 5$ , and  $6$  have been shifted along the y-axis by factors of  $0.5$ ,  $1$ , and  $0.25$  for better visibility. Please note that  $L = N - 1$  since a polymer with  $N$  monomers has  $N - 1$  “bonds.”

transmembrane domains, that is, an attractive short-ranged potential between the proteins emerges.<sup>30</sup> In the presence of such an attraction, we expect the polymer of transmembrane proteins to adopt the behavior of a two-dimensional molten globule, i.e.,  $R_g \sim L^{1/2}$ , while for vanishing hydrophobic mismatch we expect the Flory scaling  $R_g \sim L^{3/4}$ . For finite systems, it is worth noting that  $L = N - 1$  is the length of the polymer since  $N$  monomers are connected by  $N - 1$  “bonds.” Indeed, our numerical data for  $n = 4$  and  $6$  agree well with the anticipated molten-globule behavior (Fig. 2). For  $n = 5$ , the Flory exponent  $\nu = 3/4$  is not fully reached, most likely due to a small, yet still measurable hydrophobic mismatch (cf. discussion in Ref. 30) that can be expected to reduce  $\nu$  in finite systems.

This explanation is supported by results obtained for simulations in which the membrane was modeled as a thin film of single beads with a fixed  $z$ -coordinate (cf. above and Ref. 29). Neglecting the membrane’s structure in this approach, and hence any hydrophobic mismatching, the scaling for  $R_g$  indeed showed a good agreement with the anticipated Flory scaling (Fig. 2, uppermost curve).

We next studied dynamic properties by monitoring the MSD of individual transmembrane proteins and the polymers’ center of mass. The calculation of the MSD involved all monomers and was based on a combination of time and ensemble average. In particular, the MSD at time point  $t = k\Delta t$  was calculated from the positions  $r_i$  of all  $i = 1, \dots, N$  monomers within the time series of length  $j = 1, \dots, M$  with time increments  $\Delta t$

$$\langle r^2(k) \rangle = \frac{\sum_{i=1}^N \sum_{j=1}^{M-k} [r_i(j) - r_i(k+j)]^2}{N(M-k)}. \quad (1)$$

The MSD of individual monomers should exhibit three distinct temporal regimes as described in Refs. 31 and

32: an initial diffusive regime followed by an interval of subdiffusion that eventually tends toward the polymer’s center-of-mass motion. The use of soft potentials and the DPD thermostat did not allow us to observe the first regime, but the two successive regimes were accessible. Irrespective of the degree of hydrophobic mismatching we observed a subdiffusive scaling of the monomers’ MSD that eventually converged toward the (normally diffusive) MSD of the polymer’s center of mass [Fig. 3(a)]. The duration of this interval of subdiffusion depended on the polymer’s size and the degree of hydrophobic mismatching.

The determined anomaly exponents  $0.6 < \alpha < 0.7$  are in good agreement with predictions from the Rouse model with self-avoidance ( $\alpha = 3/5$ ). In all cases, the anomaly  $\alpha$  shows a slight but systematic decrease with increasing oligomer size  $N$ , and it is also sensitive to the number of transmembrane layers,  $n$ . A slight decrease of  $\alpha$  with  $N$  is anticipated for short polymers due to finite-size corrections, while for large  $N$  the anomaly is expected to remain constant. Taking into account only the four innermost monomers for the MSD did not change the anomaly significantly (data not shown).

Subdiffusion of monomers was also obtained in simulations in which the membrane was modeled as a thin liquid film (cf. above and Ref. 29). In this case the anomaly was slightly higher ( $\alpha \approx 0.8$ ), most likely due to the lack of membrane modes and the  $z$ -coordinate of membrane beads.

In any case, our numerical results on the emergence of anomalous diffusion of monomers strongly indicate that membrane-resident polymers follow Rouse dynamics rather than the Zimm model albeit hydrodynamics is taken into account explicitly. Transient subdiffusion of monomers in polymers or network structures has recently been related to fractional Brownian motion within a generalized elastic model.<sup>33</sup> Hence, anomalous motion of monomers, as seen in our simulations, can be viewed as a result of fractional Gaussian noise that renders the random walk non-Markovian.

Next, the collective motion of the protein complex was used to extract the diffusion coefficient  $D$  of the polymer’s center of mass. Concerning the scaling of the latter, the predictions of Rouse and Zimm model in two dimensions are somewhat academic as even the diffusion of simple membrane-resident cylinders suffers from the peculiar hydrodynamic divergencies in two dimensions.<sup>34</sup> Moreover, any extended membrane-embedded object can be expected to also experience a friction with the solvent surrounding the membrane.

Indeed, the polymer’s center-of-mass diffusion is well described by the famous Saffman and Delbrück relation (Fig. 4)  $D = k_B T (\ln\{h\eta_m/(R\eta_c)\} - \gamma)/(4\pi\eta_m h)$ .<sup>34</sup> This expression not only includes the thickness and viscosity of the membrane ( $h$  and  $\eta_m$ , respectively), but also takes into account the coupling of membrane inclusions to the surrounding fluid/solvent (viscosity  $\eta_c$ );  $\gamma$  is Euler’s constant. For large radii, i.e., for  $R \ll R_c = h\eta_m/\eta_c$ , the Saffman-Delbrück result does not apply any more and an asymptotic scaling  $D \sim 1/R$  emerges<sup>35</sup> in analogy to the edgewise motion of a thin disk. A fitting function  $D(R)$  for all radii was devised recently,<sup>36</sup> and we have used this expression to fit our numerical data (with  $R = R_g$ ). Our numerical data for  $n = 4, 5$ , and  $6$  are well



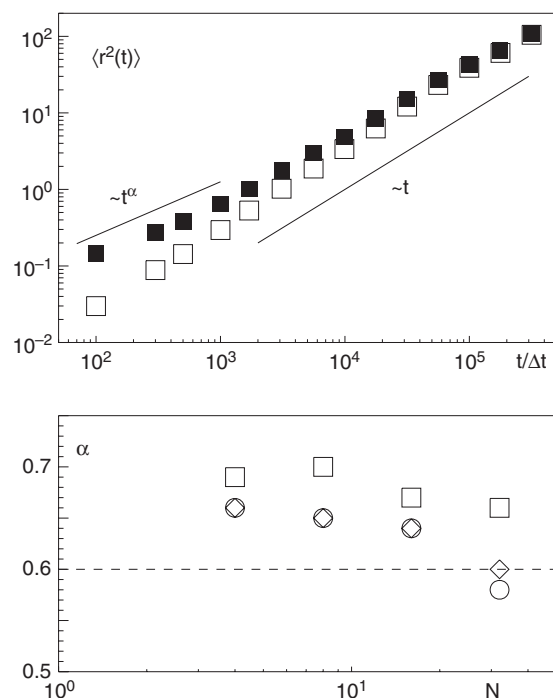


FIG. 3. (a) Mean square displacement  $\langle r^2(t) \rangle$  of a transmembrane protein within a polymer of length  $N = 16$  and vanishing hydrophobic mismatch ( $n = 5$ ; filled symbols). At early times the anticipated subdiffusion  $\langle r^2(t) \rangle \sim t^\alpha$  is observed while asymptotically the diffusion converges toward the normal diffusive MSD of the center of mass (open symbols). (b) The anomaly  $\alpha$  of the monomers' transient subdiffusion varies slightly with polymer length  $N$  and the degree of hydrophobic mismatching, yet it stays in the range  $0.6 < \alpha < 0.7$ . Open squares, circles, and diamonds denote  $n = 4, 5$ , and  $6$ , respectively.

captured by the fitting function, and the fitting parameters underline the applicability of the Saffman–Delbrück limit (i.e.,  $R_g \ll R_c$  for the shown data points). In support of this, we observed that a simple  $D \sim 1/R$  deviates strongly from the numerical data. Data for the model of a thin liquid film with fixed  $z$ -components can also be fitted well with the fitting function  $D(R)$ , yet here the parameters indicate a regime  $R_g \gg R_c$ . Indeed, the asymptotic scaling  $D \sim 1/R$  alone also provides a good fit to the numerical data (Fig. 4, inset). This result can be rationalized by recalling that the thickness of the film is  $h \approx r_0$  and its viscosity is similar to that of the surrounding solvent ( $\eta_m \approx \eta_c$ ). Hence,  $R_c \approx r_0$  and only the asymptotic dependence  $D(R) \sim 1/R$  can be seen for this model.

In summary, we have shown that the center-of-mass diffusion of linear polymers of transmembrane proteins is well described by the Saffman–Delbrück relation while monomers show a transient subdiffusion. The latter result is in good agreement with predictions of the Rouse model. Rouse-like dynamics is somewhat surprising as our simulations included hydrodynamic interactions. Most likely the coupling of membrane inclusions to the solvent around the bilayer rather than the mere complexity of the membrane is the crucial ingredient for the emergence of the monomers' subdiffusion since both simulation approaches yielded anomalous diffusion.

Although we have studied here only fairly short protein polymers, we expect our results to hold also for larger

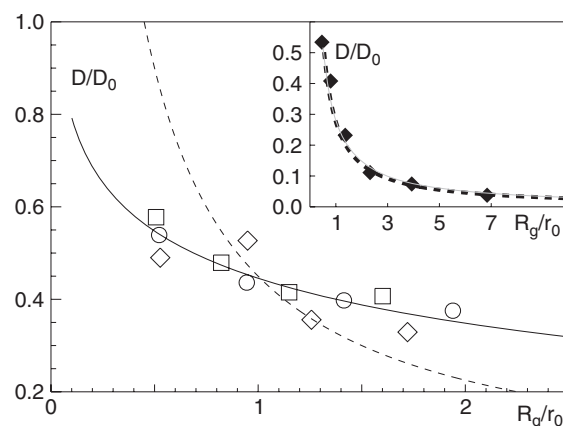


FIG. 4. The center-of-mass diffusion coefficient  $D$  of a polymer of transmembrane proteins is well described by the Saffman–Delbrück relation (full line). Here,  $R_g$  is the polymer's radius of gyration, and  $D_0$  is the diffusion constant for a single lipid in the bilayer. In contrast, fitting an expression  $D \sim 1/R_g$  (dashed line) to the numerical data reveals major deviations. Open squares, circles, and diamonds denote  $n = 4, 5$ , and  $6$ , respectively. Inset: A good agreement with Saffman–Delbrück is also found when modeling the membrane as a thin liquid layer with a fixed  $z$ -coordinate (full gray line), yet also a simple  $D \sim 1/R_g$  relation (dashed line) compares favorably to the data. The reason for the latter finding is the special setting of the simulation that reduces the applicability of the classical Saffman–Delbrück theory (see main text for details).

oligomers. We would like to put forward two reasons why the observed scaling is meaningful and most likely unaffected by finite-size effects. First, the scaling of the MSD with an apparent anomaly exponent  $\alpha$  is an experimentally measurable quantity also for short polymers. Even if the asymptotic scaling arguments were not valid, an experimental observation of  $\alpha < 1$  would require an explanation. Our study provides such an explanation. Second, we tested by means of Brownian dynamics (i.e., without explicit solvent particles) how well the Flory scaling  $R_g \sim N^\nu$  in two dimensions ( $\nu = 0.75$ ) is recovered even for small polymers. Using polymers with  $N = 4, \dots, 256$ , we found a scaling exponent  $\nu = 0.775 \pm 0.025$  that compares favorably to the theoretical prediction. For this data set, we did not observe a systematic deviation from the scaling for polymers with  $N < 50$ . On this basis, we also expect finite-size corrections of the anomaly to be mild, even for the case with explicit solvent.

Since modern microscopy methods rely on quantifying the diffusion of individual, fluorescently labeled proteins, our results provide an explanation for the previously observed subdiffusion of glycosylation enzymes on intracellular membranes.<sup>6</sup> Indeed, the experimentally observed anomalies  $0.55 < \alpha < 0.85$  compare favorably to the anomaly observed here for monomer motion. Indeed, membrane-resident glycosylation enzymes have been predicted,<sup>37</sup> and at least in part been shown<sup>3</sup> to form higher-order structures that are most likely linear polymers. Subdiffusion of such structures was seen on time scales  $t < 100$  ms (Ref. 6) with the anticipated polymers involving up to 100 monomers.<sup>3</sup> On the basis of our findings, the crossover time from the monomers' subdiffusion toward the (normal) center-of-mass diffusion is expected to follow the scaling of the Rouse relaxation time  $\tau \sim N^{1+2\nu}$ . Given that the crossover time for a polymer of length  $N = 16$

roughly occurs at  $t = 10^5 \Delta t \approx 10 \mu\text{s}$  (Fig. 3), a polymer with 100 monomers may be expected to show transient subdiffusion at least up to  $\sim 500 \mu\text{s}$ . Indeed, this time scale is well within the experimentally observed range.<sup>6</sup> Shortcomings of our simulation approach (simplified model, nonvanishing hydrophobic mismatch, finite-size corrections, and the almost equivalent speed of momentum and mass transport inherent to DPD) may explain the somewhat too early crossover to normal diffusion in the simulation as compared to experiments.

It is also noteworthy that the experimentally observed subdiffusion of these enzymes in principle could also be due to other mechanisms, e.g., obstructed diffusion/percolation due to (lipid- or protein-based) molecular crowding. However, a recent extensive Monte Carlo approach<sup>38</sup> and percolation theory in two dimensions<sup>39</sup> put up a lower bound  $\alpha > 0.69$  that contradicts the experimentally observed anomalies  $\alpha < 0.7$  (cf. also discussion in Ref. 6). Transient interactions that enforce power-law distributed resting times between periods of free diffusion (“continuous time random walk”) seem unlikely as this scenario would have to rely on the continuous consumption of energy.<sup>40</sup> By process of elimination, we therefore propose that membrane-resident glycosylation enzymes display anomalous diffusion properties due to their dynamic oligomerization properties, in accordance with our above simulations.

## ACKNOWLEDGMENTS

This work was supported by the Institute for Modeling and Simulation in the Biosciences (BIOMS) in Heidelberg. U.S. was funded by the FORSYS initiative (VIROQUANT) from the German Federal Ministry of Education and Research.

<sup>1</sup>S. Schuck and K. Simons, *J. Cell. Sci.* **117**, 5955 (2004).

<sup>2</sup>P. Park, S. Filipek, J. Wells, and K. Palczewski, *Biochemistry* **43**, 15643 (2004).

<sup>3</sup>D. M., K. Dejgaard, J. Füllekrug, S. Dahan, A. Fazel, J. Paccaud, D. Thomas, J. Bergeron, and T. Nilsson, *J. Cell. Biol.* **140**, 751 (1998).

<sup>4</sup>G. Schutz, H. Schindler, and T. Schmidt, *Biophys. J.* **73**, 1073 (1997).

<sup>5</sup>P. Smith, I. Morrison, K. Wilson, N. Fernandez, and R. Cherry, *Biophys. J.* **76**, 3331 (1999).

<sup>6</sup>M. Weiss, H. Hashimoto, and T. Nilsson, *Biophys. J.* **84**, 4043 (2003).

<sup>7</sup>K. Ritchie, X. Shan, J. Kondo, K. Iwasawa, T. Fujiwara, and A. Kusumi, *Biophys. J.* **88**, 2266 (2005).

<sup>8</sup>M. Wachsmuth, W. Waldeck, and J. Langowski, *J. Mol. Biol.* **298**, 677 (2000).

<sup>9</sup>M. Weiss, M. Elsner, F. Kartberg, and T. Nilsson, *Biophys. J.* **87**, 3518 (2004).

<sup>10</sup>D. Banks and C. Fradin, *Biophys. J.* **89**, 2960 (2005).

<sup>11</sup>G. Guigas, C. Kalla, and M. Weiss, *Biophys. J.* **93**, 316 (2007).

<sup>12</sup>M. Saxton, *Biophys. J.* **66**, 394 (1994).

<sup>13</sup>W. Deng and E. Barkai, *Phys. Rev. E* **79**, 011112 (2009).

<sup>14</sup>R. Metzler and J. Klafter, *Phys. Rep.* **339**, 1 (2000).

<sup>15</sup>J. Szymanski and M. Weiss, *Phys. Rev. Lett.* **103**, 038102 (2009).

<sup>16</sup>M. Magdziarz, A. Weron, K. Burnecki, and J. Klafter, *Phys. Rev. Lett.* **103**, 180602 (2009).

<sup>17</sup>V. Tejedor, O. Benichou, R. Voituriez, R. Jungmann, F. Simmel, C. Selhuber-Unkel, L. Oddershede, and R. Metzler, *Biophys. J.* **98**, 1364 (2010).

<sup>18</sup>R. Shusterman, S. Alon, T. Gavrinov, and O. Krichevsky, *Phys. Rev. Lett.* **92**, 048303 (2004).

<sup>19</sup>B. Maier and J. Rädler, *Phys. Rev. Lett.* **82**, 1911 (1999).

<sup>20</sup>A. G. Zilman and R. Granek, *Phys. Rev. E* **58**, R2725 (1998).

<sup>21</sup>T. Tlusty, *Macromolecules* **39**, 3927 (2006).

<sup>22</sup>P. J. Hoogerbrugge and J. M. V. A. Koelman, *Europhys. Lett.* **19**, 155 (1992).

<sup>23</sup>P. Español and P. Warren, *Europhys. Lett.* **30**, 191 (1995).

<sup>24</sup>R. D. Groot and P. B. Warren, *J. Chem. Phys.* **107**, 4423 (1997).

<sup>25</sup>M. Laradji and P. B. S. Kumar, *Phys. Rev. Lett.* **93**, 198105 (2004).

<sup>26</sup>P. Nikunen, M. Karttunen, and I. Vattulainen, *Comput. Phys. Commun.* **153**, 407 (2003).

<sup>27</sup>A. F. Jakobsen, *J. Chem. Phys.* **122**, 124901 (2005).

<sup>28</sup>A. F. Jakobsen, O. G. Mouritsen, and M. Weiss, *J. Phys.: Condens. Matter* **17**, S4015 (2005).

<sup>29</sup>S. Ramachandran, S. Komura, and G. Gompper, *EPL* **89**, 56001 (2010).

<sup>30</sup>U. Schmidt, G. Guigas, and M. Weiss, *Phys. Rev. Lett.* **101**, 128104 (2008).

<sup>31</sup>K. Kremer and G. S. Grest, *J. Chem. Phys.* **92**, 5057 (1990).

<sup>32</sup>W. H. Jiang, J. H. Huang, Y. M. Wang, and M. Laradji, *J. Chem. Phys.* **126**, 044901 (2007).

<sup>33</sup>A. Taloni, A. Chechkin, and J. Klafter, *Phys. Rev. Lett.* **104**, 160602 (2010).

<sup>34</sup>P. G. Saffman and M. Delbrück, *Proc. Natl. Acad. Sci. U.S.A.* **72**, 3111 (1975).

<sup>35</sup>B. D. Hughes, B. A. Pailthorpe, and L. R. White, *J. Fluid Mech.* **110**, 349 (1981).

<sup>36</sup>E. Petrov and P. Schwille, *Biophys. J.* **94**, L41 (2008).

<sup>37</sup>T. Nilsson, P. Slusarewicz, M. Hoe, and G. Warren, *FEBS Lett.* **330**, 1 (1993).

<sup>38</sup>D. Nicolau, Jr., J. Hancock, and K. Burrage, *Biophys. J.* **92**, 1975 (2007).

<sup>39</sup>J. P. Bouchaud and A. Georges, *Phys. Rep.* **195**, 127 (1990).

<sup>40</sup>M. Saxton, *Biophys. J.* **92**, 1178 (2007).